

Articles

Field Effect Studies on Rubrene and Impurities of Rubrene

Roswitha Zeis,[†] Celine Besnard,[‡] Theo Siegrist,^{†,‡} Carl Schlockermann,[†] Xiaoliu Chi,[†] and Christian Kloc^{*,†}

*Bell Laboratories, Lucent Technologies, 600 Mountain Avenue, Murray Hill, New Jersey 07974, and
Department of Materials Chemistry, Lund University, S-221 00 Lund, Sweden*

Received February 3, 2005. Revised Manuscript Received November 17, 2005

Rubrene single crystals have been grown by a vapor-phase process. Two additional compounds that contaminate rubrene have been identified and their structures determined. Single crystals of rubrene show excellent crystallinity and very small rocking curve width. Field effect transistors based on pure rubrene single crystals with colloidal graphite electrodes and Parylene as a dielectric demonstrate a maximal mobility of 13 cm²/Vs with strong anisotropy. The mobility increases very slightly with cooling, but decreases significantly at low temperatures.

1. Introduction

Rubrene is distinguished from other known organic semiconductors by an exceptionally high carrier mobility of 30 cm²/Vs at 200 K¹ in field effect transistors fabricated from single crystals. While pentacene and related acenes, oligothiophenes, and fullerenes are the most studied organic FET materials today, they have mobilities almost 10 times lower than that of rubrene.^{2,3} The carrier transport mechanism in all of these organic semiconductors is still not well understood. For example, the contributions of defects and phonon scattering remain to be identified for each system, though recently, progress has been made for pentacene.⁴ The presence of defects in organic semiconducting single crystals and the immaturity of organic FET technology seem to limit understanding of transport processes in π electron systems. In particular, the fundamental limits of the room-temperature mobility and why the mobility in organic semiconductors does not increase dramatically upon cooling as in most inorganic semiconductors must be further explored. Therefore, further study of the material factors important for operation of rubrene single-crystal FETs may contribute to the improvement of organic FETs and ultimately lead to the design of compounds with the desired properties.

Rubrene has many advantages and it is commercially available. When grown from the vapor phase, rubrene forms large, orthorhombic, high-quality crystals characterized by

a small mosaic spread. High FET mobility values have been reproduced in several laboratories using different crystal growth and FET preparation methods.^{1–8} In this paper, we are reporting only on rubrene single-crystal FETs where Parylene is used as the gate dielectric. The FET mobility values obtained from many measured transistors are reproducible, are nearly gate voltage independent, and are slightly increased upon cooling. A pronounced anisotropy of the mobility with respect to the crystal orientation was observed.

Since impurities formed during the growth process or as byproducts of the commercial powder synthesis can seriously degrade the electronic transport properties of the crystals and devices,^{9,10} we studied the processes occurring in single-crystal growth. Besides rubrene, we have identified two additional compounds present in the growth process. We determined their crystal structures, and because they prove to be aromatic like rubrene, we studied their field effect transistor behavior.

2. Experimental Section

We grew rubrene single crystals by horizontal physical vapor transport in a flow of argon gas as we reported previously.¹¹ The source, containing the rubrene powder acquired from Aldrich, was

* To whom correspondence should be addressed. E-mail: ckloc@lucent.com.

[†] Lucent Technologies.

[‡] Lund University.

- (1) Podzorov, V.; Menard, E.; Borissov, A.; Kiryukhin, V.; Rogers, J. A.; Gershenson, M. E. *Phys. Rev. Lett.* **2004**, *93*, 086602.
- (2) de Boer, R. W. I.; Gershenson, M. E.; Morpurgo, A. F.; Podzorov, V. *Phys. Status Solidi* **2004**, *A201*, 1302.
- (3) Goldmann, C.; Haas, S.; Krellner, C.; Pernstich, K. P.; Grundlach, D. J.; Batlogg, B. *J. Appl. Phys.* **2004**, *96*, 2080.
- (4) Lang, D. V.; Chi, X.; Siegrist, T.; Sargent, A. M.; Ramirez, A. P. *Phys. Rev. Lett.* **2004**, *93*, 076601.

- (5) Strassen, A. F.; de Boer, R. W. I.; Iosad, N. N.; Morpurgo, A. F. *Appl. Phys. Lett.* **2004**, *85*, 3899.
- (6) Butko, V. Y.; Lashley, J. C.; Ramirez, A. P. *Phys. Rev. B* **2005**, *72*, 081312.
- (7) Sundar, V. C.; Zaumseil, J.; Podzorov, V.; Menard, E.; Willett, R. L.; Someya, T.; Gershenson, M. E.; Rogers, J. A. *Science* **2004**, *303*, 1644.
- (8) Podzorov, V.; Sysoev, S. E.; Loginova, E.; Pudalov, V. M.; Gershenson, M. E. *Appl. Phys. Lett.* **2003**, *83*, 3504.
- (9) Roberson, L. B.; Kowalik, J.; Tolbert, L. M.; Kloc, C.; Zeis, R.; Chi, X.; Fleming, R.; Wilkins, C. J. *Am. Chem. Soc.* **2005**, *127*, 3069.
- (10) Jurchescu, O. D.; Baas, J.; Palstra, T. T. M. *Appl. Phys. Lett.* **2004**, *84*, 3061.
- (11) Laudise, R. A.; Kloc, C.; Simpkins, P. G.; Siegrist, T. *J. Cryst. Growth* **1998**, *187*, 449.

heated to 280 °C in the hot zone of a two-zone furnace while the second zone of the furnace was held at 200 °C. Rubrene single crystals nucleated spontaneously on the wall of the glass tube in the colder zone of the furnace and grew as elongated flat red needles or platelets that were several millimeters long with a thickness ranging from 10 to 500 μm . In the very coldest part of the reaction tube, near the end of the furnace, a yellow deposit was observed. Some already sublimed rubrene crystals were further used for a vacuum-sealed ampule growth. This last procedure resulted in crystals growing in smaller temperature gradients close to thermodynamic equilibrium and produced thicker crystals, useful for anisotropy measurements.

All the crystal structures reported in this paper were determined using an Oxford-Diffraction Xcalibur-2 diffractometer, and rocking curves were either measured in triple-axis mode on a custom 4-circle diffractometer with copper radiation and LiF monochromator or on a Bruker D8 Discover diffractometer. Rubrene crystallizes in an orthorhombic unit cell, space group *Cmca*, and $a = 26.901$ Å, $b = 7.187$ Å, and $c = 14.430$ Å. Atomic force microscope (AFM) images were obtained with a customized setup based on a Nanonix AFM head and Oxford Tops 3 controller. The setup was calibrated with a 22 nm step reference. On the surface of freshly grown crystals, a typical field effect transistor structure was produced using a technique described previously by Podzorov et al.¹² Source and drain contacts were painted with a water-based solution of colloidal graphite. The channel lengths, l , and width, w , were determined by dimensions of crystals and electrode painting process and were typically in the range of $l = 0.5$ mm and $w = 1$ mm. The gate-insulating layer consisted of a 1.1–1.7 μm Parylene N thin film. Perylene films were deposited on crystals of rubrene with source–drain electrodes at room temperature from commercial dimmer which decomposed at a 680 °C zone to monomer.¹² The thickness of these films was determined with a profilometer. On top of the parylene layer, between source and drain, the gate electrodes were painted with colloidal graphite. The channel capacitance was calculated from the thickness of the insulating layer and the tabulated dielectric constant of Parylene N ($\epsilon_r = 2.65$). At room temperature the transistor characteristics were measured using an HP test fixture connected to an HP 4145B semiconductor parameter analyzer. The low-temperature measurements were performed in a helium atmosphere in a Quantum Design cryostat with a secondary Pt100 resistor in proximity to the sample to cross-check the temperature.

3. Results and Discussion

During the crystal growth process, we observed that small pale yellow needlelike crystals also formed downstream from red rubrene crystals. We collected these impurities and used them to further gas-phase crystal growth. An X-ray structure analysis was performed, and we identified two rubrene related molecules. Compound A ($\text{C}_{42}\text{H}_{30}$) is richer and compound B ($\text{C}_{42}\text{H}_{26}$) is poorer in hydrogen than rubrene ($\text{C}_{42}\text{H}_{28}$). The molecular structures of both molecules A and B are shown in Figure 1.

Compound A, $\text{C}_{42}\text{H}_{30}$, has been reported to form by the reaction of diaryl 1,1-dibromoethylene with active metallic nickel,¹³ and we found traces of it in the commercial rubrene. The synthetic procedure used for the commercial rubrene is unknown to us and we cannot explain the origin of A, which

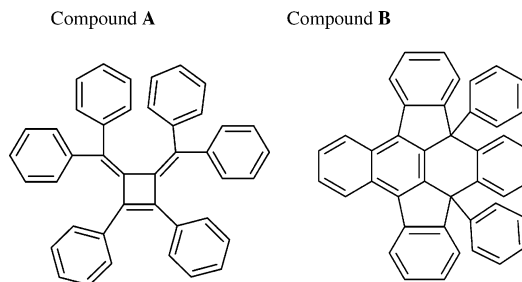


Figure 1. Molecular structures of compounds separated from rubrene during crystal growth process. Compound A ($\text{C}_{42}\text{H}_{30}$) and compound B ($\text{C}_{42}\text{H}_{26}$). Details of crystal structures are available in the Supporting Information.

appears to be an unlikely product of the older preparation method.¹⁴

Compound A crystallizes in a monoclinic unit cell with space group $P2_1/n$. Six phenyl groups are present around the cyclobutadiene, four of them attached two by two to an intermediate carbon atom. The planes formed by these rings are at different angles out of the plane of the central four-atom ring.

The phenyl groups of molecule A show quite a large deviation from being parallel. This can be explained by the molecular packing in which the phenyl groups are avoiding each other. Although the phenyl groups are oriented at different angles, the molecule stays reasonably flat and forms a layer. The molecular packing is obtained by applying 2_1 symmetry that forms parallel layers perpendicular to the b -axis. A remarkably short carbon–carbon intermolecular distance (3.49 Å) occurs between molecules in the plane. The shortest distance between two parallel planes is 3.52 Å. This distance occurs between a carbon of the four-member rings and a carbon of a phenyl group.

Compound B, $\text{C}_{42}\text{H}_{26}$, has two hydrogen atoms less than rubrene, suggesting an oxidation reaction taking place during the growth process. This may be possible because the argon carrier gas that we use for crystal growth contains a few ppm of oxygen. The structure of the molecule can be derived from a thermal cyclization reaction of rubrene involving fusing two phenyl rings to the tetracene backbone. This arrangement breaks the extended aromatic system of the tetracene, producing curvature. The molecule is quite bulky due to two remaining phenyl groups that are pointing outward. To take care of these and pack as efficiently as possible, the molecules associate pairwise in the crystal, turning the phenyl groups in opposite directions. The distance between two molecules in such a dimer is 3.52 Å, and there is a short contact of the two molecules via two phenyl groups.¹⁵

We prepared single-crystal field effect transistors on the surfaces of crystals of both compounds, A and B, in a method similar to the one described above for rubrene. We observed field effect transistor activity in the crystals of A but not of B. At room temperature, the field effect transistor exhibits an on/off ratio larger than 10^4 . From the saturation regime we determined a hole mobility of around $2.3 \times 10^{-2} \text{ cm}^2/\text{Vs}$. In compound A, every second carbon–carbon bond is a

(12) Podzorov, V.; Pudalov, V. M.; Gershenson, M. E. *Appl. Phys. Lett.* **2003**, 82, 1739.

(13) Iyoda, M.; Mizusuna, A.; Oda, M. *Chem. Lett.* **1988**, 1, 149.

(14) Doge, J. A.; Bain, J. D.; Chamberlin, A. R. *J. Org. Chem.* **1990**, 55, 4190.

(15) Besnard, C. Ph.D. Thesis, University of Lund, Lund, Sweden, 2004.

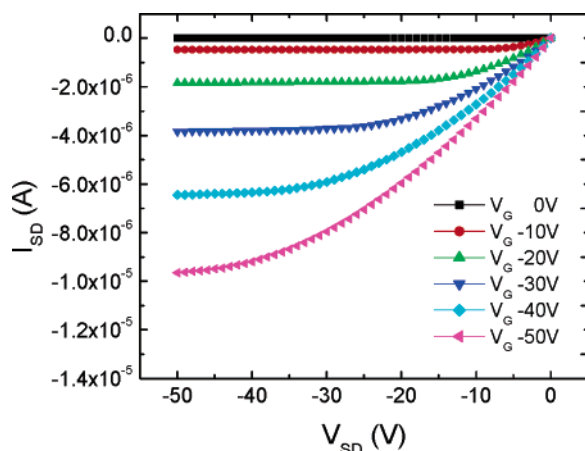


Figure 2. Output characteristics of a rubrene single-crystal FET.

double bond, and the molecule has 21 π electron pairs. From 42 carbon atoms, every carbon atom is sp^2 hybridized and is a source of π electrons. In contrast, compound B, with the same number of carbon atoms, has 20 π electron pairs and the sp^2 hybridization of two from 42 carbon atoms has been lost. We believe that this causes delocalization of π electrons only on a part of molecule B. Therefore, B does not show any field effect activity whatsoever.

The quality of the rubrene crystals has been assessed by measuring X-ray rocking curves. A single peak of the (600) Bragg reflection was observed with the full-width at half-maximum of around 0.016° , indicating a small mosaic spread in the crystals. This value is about a factor of 5 smaller than in other organic crystals, such as pentacene.¹⁶ It is not clear if the low mosaicity is connected with the high symmetry (orthorhombic) of rubrene crystals, but the agreement between high mobility and high crystalline perfection in rubrene is remarkable.

At room temperature, we routinely achieved carrier mobilities above $1 \text{ cm}^2/\text{Vs}$ on numerous rubrene crystals from different batches. The highest mobility obtained in our study was $13 \text{ cm}^2/\text{Vs}$, as derived from the saturation region. This value is slightly less than reported FET mobilities obtained using PDMS stamps on rubrene single crystals, but it is still exceptionally high compared to other organic single crystals, like pentacene ($2.2 \text{ cm}^2/\text{Vs}$)⁹ and tetracene ($1.3 \text{ cm}^2/\text{Vs}$).³ Besides the high field effect mobilities, our devices showed small threshold voltages V_{TH} (below 1 V), a relatively large on/off ratio of 10^5 and a sharp field effect onset ($S_1 = 3\text{--}8 \text{ nF/decade}\cdot\text{cm}^{-2}$). In Figure 2 the output characteristic of such an FET is presented. Additionally, nearly all transistors showed a quadratic dependence of the saturation current versus the gate bias ($V_G^x \propto I_{\text{SDsat}}$ for $x \sim 1.8\text{--}2.1$) (Figure 3) and linear behavior of the source–drain current for gate bias $V_G < |V_{\text{SD}} - V_{\text{T}}|$ ($V_G^x \propto I_{\text{SD}}$, $x \sim 0.8\text{--}1.1$). These FET features imply ohmic source and drain contacts. This goes along with the fact that for a sufficiently large gate- and source–drain bias (-20 V), the carrier mobility is independent of the longitudinal field (source–drain voltage) and only weakly dependent on the transverse field (gate voltage) (Figure 4). For $V_{\text{SD}} = V_G$, a peak in mobility and decrease

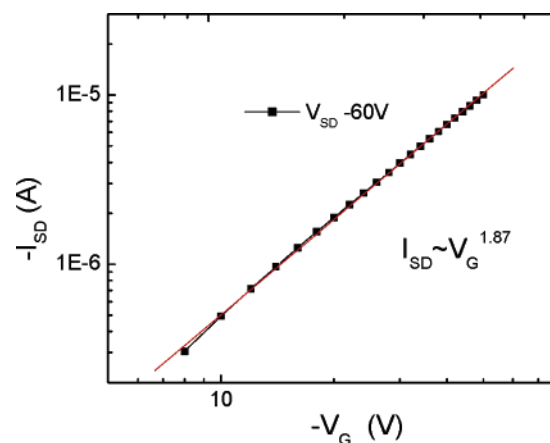


Figure 3. Dependency of the saturation current on the gate bias.

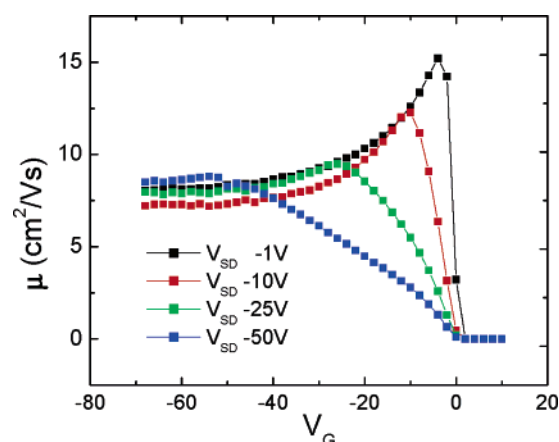


Figure 4. Mobility versus the gate voltage (calculated from the linear regime).

of mobility with increasing gate voltage is observed. This peak is predominant in the crystals showing the highest mobility. Such a dependency was not observed in any other organic material since the mobility in other materials was significantly lower than in rubrene. It is possible that the high quality of rubrene FETs allows us to see the first indications of channel narrowing. Such an effect has already been observed in inorganic FETs¹⁷ where mobility is much higher. The lack of pronounced mobility increase upon cooling, however, prevents us from definitely excluding the contact effect on the conductivity of the channel.

Due to the anisotropy of the crystal structure and direction-dependent overlap of the π electrons, the charge transport properties of molecular crystals are expected to be anisotropic. Anisotropy has been observed in time-of-flight measurements¹⁸ in anthracene single crystals and on single-crystal rubrene FETs using PDMS stamps⁷ to make contacts. To study the anisotropy of a rubrene single crystal, we choose a source and drain contact configuration as shown in Figure 5. Such configuration allows us to measure three field effect transistors in two different crystallographic directions on the same crystal. We picked a thick crystal grown close to equilibrium in a sealed ampule. Four contacts in the configuration presented in Figure 5 served alternatively as

(16) Siegrist, T. Unpublished work.

(17) Sze, S. M. *Physics of Semiconductor Devices*, 2nd ed.; John Wiley & Sons: New York, 1991.

(18) Karl, N.; Marktanner, J. *Mol. Cryst. Liq. Cryst.* **2001**, 355, 149.

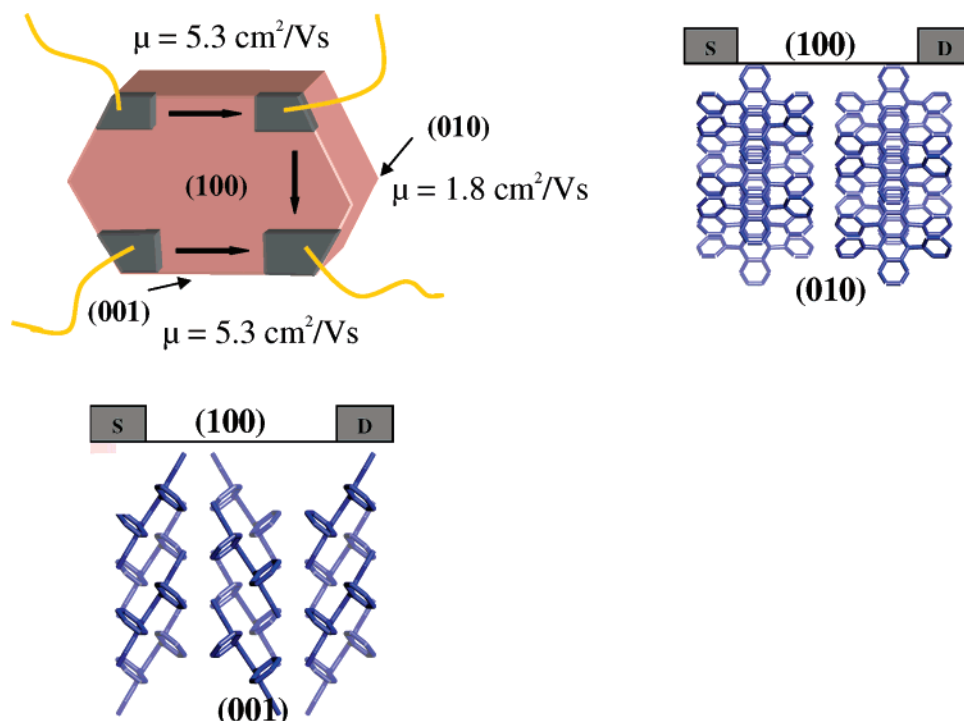


Figure 5. (a) Source–drain contact configuration to measure the mobility in different crystallographic directions. (b) Crystallographic structure along the *b* direction. (c) Crystallographic structure along the *a* direction.

source or drain electrodes. The whole crystal (100) face was covered by a Parylene layer, and between each two electrodes, a gate contact was placed (not shown on Figure 5). Within the (100) plane, the highest mobility ($5.3 \text{ cm}^2/\text{Vs}$) was observed along the *b* direction, which is consistent with the molecular packing in the rubrene crystal. The π electron overlap of the adjacent molecules in the *b* direction is the highest, and the mobility is 3 times greater along the *b*-direction than along the *c*-axis. For comparison, V. Podzorov et al.⁷ reported a ratio of anisotropy between 2.5 and 3.

The source–drain current flows in a thin surface layer. Therefore, it is possible that growth steps formed during crystal layer-by-layer growth are responsible for the observed anisotropy. We performed AFM measurements on the rubrene (100) face and observed 1.3–1.4 nm high monolayer steps separated by 600 nm wide terraces. However, larger step free regions up to $3 \mu\text{m}$ were also observed. These measurements show an excellent molecular smoothness of rubrene surfaces and we conclude that the observed anisotropy results from the bulk orientation of molecules and not from any anisotropy of the steps on the crystal surface.

The temperature dependence of the field-effect mobility of one rubrene sample is shown in Figure 6. Over the range $250 \text{ K} < T < 300 \text{ K}$ we observe a slight increase of the mobility with decreasing temperature. The gain in mobility is $\approx 15\%$ from 6.5 to $7.5 \text{ cm}^2/\text{Vs}$. Such a small increase in mobility upon cooling, or a temperature-independent mobility followed by radical decrease at lower temperatures, was typical for our rubrene FETs. Podzorov et al.¹ described a larger mobility increase with cooling (of approximately 50%), which may be explained by the fact that our deposition of Parylene on the single-crystal surface causes more defects in the channel than in Podzorov's stamp contact measure-

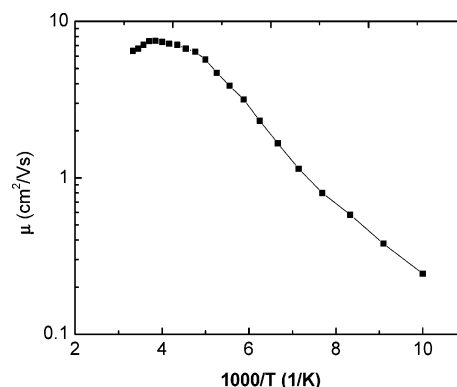


Figure 6. Temperature dependence of the carrier mobility (Arrhenius plot).

ments. A similar observation of anisotropy of mobility and increase of mobility with cooling was attributed by Podzorov et al.¹ to the signatures of intrinsic transport.

Conclusions

In a rubrene crystal growth system, two impurities resembling rubrene have been identified. One has more π electrons than rubrene and shows field effect activity, and the second has only two π electrons less and is FET inactive. Rubrene single crystals grown from purified material show excellent crystallinity and a very small rocking curve width. Field effect transistors made with pure rubrene single crystals using colloidal graphite electrodes and Parylene as a dielectric demonstrate a maximum mobility of $13 \text{ cm}^2/\text{Vs}$ and strong anisotropy. The mobility increases slightly with cooling, but drops significantly at low temperatures. We were able to reproduce many of the rubrene transistor features previously observed by other authors but further technological progress is required for a better understanding of the physics of rubrene devices.

Acknowledgment. We thank A. Ramirez and E. A. Chandross for valuable discussion, Prof. E. Bucher for his support and advice, and C. G. MacLennan for reading the manuscript. R. Zeis acknowledges financial support from the Konrad Adenauer Foundation, the German Academic Exchange Service (DAAD), and the Landesgraduiertenfoerderung Baden-Wuerttemberg. C. Besnard acknowledges support from the Swedish Science Council and C. Schlockermann acknowledges the

financial support of Deutsche Studienstiftung. We acknowledge the support of the U.S. Department of Energy under Grant No. 04SCPE389.

Supporting Information Available: Crystal structures of compounds A and B (CIF). This material is available free of charge via the Internet at <http://pubs.acs.org>.

CM0502626